Available online at www.sciencedirect.com
SCIENCE DIRECT®

Journal of the European Ceramic Society 23 (2003) 2717–2720

www.elsevier.com/locate/jeurceramsoc

A compact lumped-element lowpass filter using low temperature cofired ceramic technology

Sung-Hun Sim[a,b], Chong-Yun Kang[a], Ji-Won Choi[a,*], Hyung-Wook Choi[c], Young-Joong Yoon[b], Seok-Jin Yoon[a], Hyun-Jai Kim[a]

[a]*Thin Film Research Center, KIST, Seoul, 136-791, South Korea*
[b]*Department of Electrical & Electronics Eng. Yonsei Univ., Seoul, 120-749, South Korea*
[c]*Department of Electrical & Information/Electronic Eng. Kyungwon Univ., Kyunggi, 461-701, South Korea*

Abstract

The design method for a small lowpass filter (LPF) having a multilayer structure, which can be embedded in RF modules, is presented. Low loss, three dimensional inductors and capacitors have been investigated and incorporated to design a chip-type LPF. The Chebyshev LPF has been designed with a cutoff frequency of 2 GHz, a ripple of 0.1 dB, and a high attenuation (<-30 dB). The low temperature cofired ceramic (LTCC) materials have a dielectric constant of 7.8, a loss tangent of 0.0015, and a metallization of silver. The characteristics of the embedded passives (of which the structures were rectangular helical inductors and parallel-plate capacitors) have been analyzed by 3D structure simulator and the equivalent circuit simulated.

Keywords: LTCC; Filters; Lowpass filters

1. Introduction

Recently, the handsets for mobile communications have become very popular and miniaturization is essential. Thus, several technologies have been developed to miniaturize RF and microwave components, circuits, and system.[1–3] Among them, low temperature co-fired ceramic (LTCC) technology enables size reduction of microwave devices by fabrication in two or multilayer configurations. Several kinds of multilayer microwave devices have been developed and design methods and fabrication procedures reported.[4–7] Hence, they can be easily incorporated in the design of a variety of RF components such as voltage controlled oscillators (VCOs), power amplifiers (PAs), and mixers.

In this paper, an approach for the design of a chip-type lowpass filter (LPF) using a multilayer structure is presented. The design method for the chip-type LPF is developed using the equivalent circuit of a Chebyshev model. By employing the proposed design method, the multilayer chip LPF configuration can be made more compact and flexible. The designed chip-type LPF was realized by implementing the multilayer chip inductors and capacitors. Each lumped element was implemented using ceramic material and Ag metal layers. The dielectric constant and loss tangent was chosen to be 7.8 and 0.0043, respectively for 3D structure design of the MLC chip LPF.

This paper presents the experimental results showing the changing of the frequency characteristics with a lumped-element value. The simulated results for the designed chip-type LPF show a validation of the proposed design method.

2. Equivalent circuit of Chebyshev LPF (Lowpass filter)

Fig. 1 shows the equivalent circuit of Chebyshev LPF, with a passband ripple of 0.1 dB and a cutoff frequency of 2 GHz. The circuit consists of two series inductors

* Corresponding author. Tel.: +82-2-958-5556; fax: +82-2-958-6851.
E-mail address: jwchoi@kist.re.kr (J.-W. Choi).

0955-2219/03/$ - see front matter © 2003 Elsevier Ltd. All rights reserved.
doi:10.1016/S0955-2219(03)00184-5

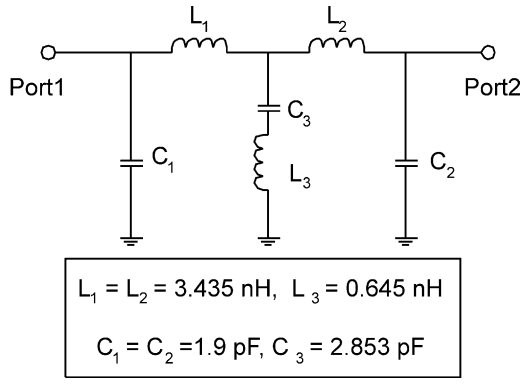

Fig. 1. Equivalent circuit of LPF with attenuation pole.

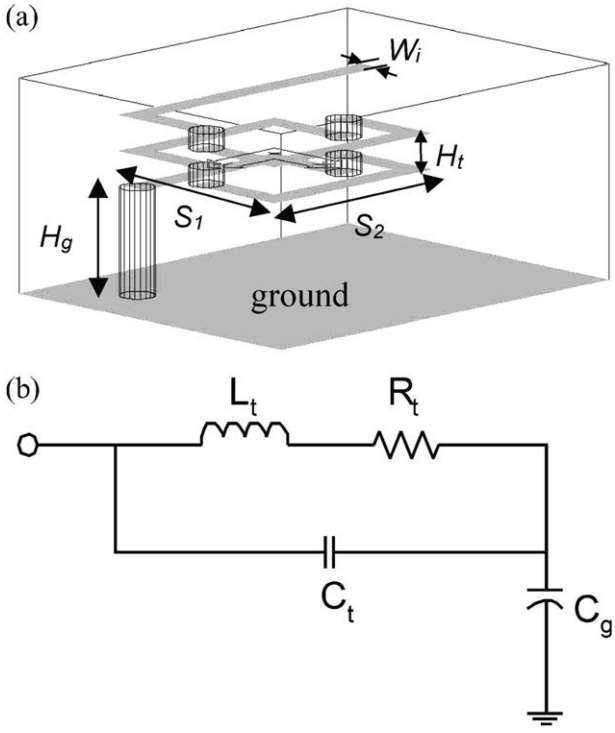

Fig. 2. The structure (a) and equivalent circuit (b) of the embedded inductor.

and two shunt capacitors, and a series resonator is designed in order to enhance the stopband characteristics of the LPF. For the equivalent circuit shown in Fig. 1, the component values are simply given by the equations of a Chebyshev model.[8]

3. Analysis of the embedded lumped elements

Prior to designing the structure of MLC chip LPF, design and analysis of the embedded passives must be completed. They are based on a ceramic with a dielectric

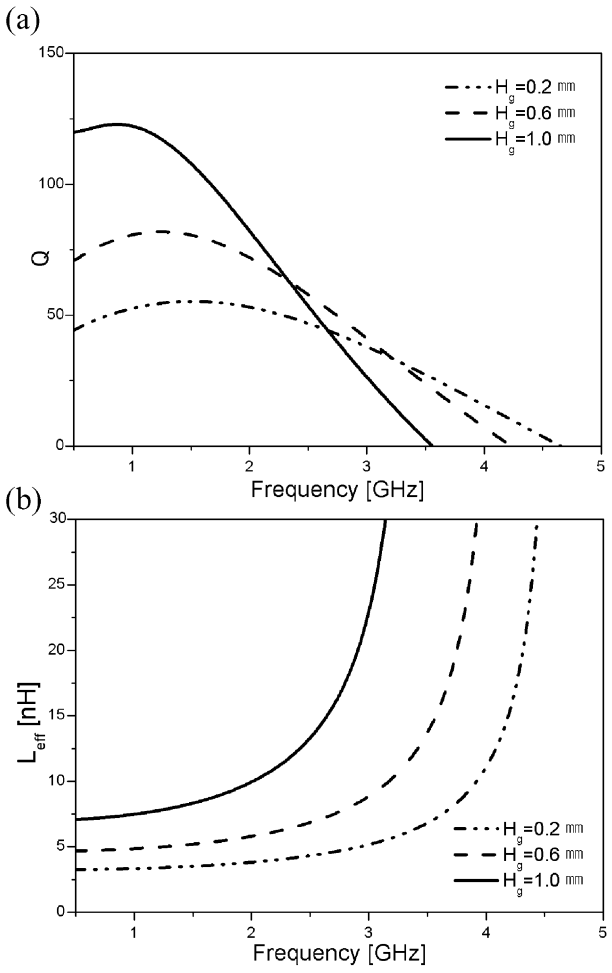

Fig. 3. The frequency characteristics of the embedded inductor ($W_1 = 0.15$ mm, $S_1 = S_2 = 1.2$ mm, $H_t = 0.2$ mm, $n = 2$ turns).

constant 7.8 and tangent loss 0.0043. The embedded inductor with multilayer configuration is based on rectangular helical structure, as shown in Fig. 2(a). The standard high frequency equivalent circuit model of the embedded inductor is shown in Fig. 2(b). The L_t, R_t, and C_t represent the inductance, the loss, and parasitic capacitance in the rectangular helix; C_g represents the parasitic capacitor coupled with the ground plane. The quality factor Q and effective inductance L_{eff} tend to change because of parasitic capacitances such as C_g and C_t of the equivalent circuit [Fig. 2(b)]. Accordingly, the inductive structure is designed to suppress these parasitic capacitors in order to improve the inherent properties of the inductor such as L_{eff} and Q.

Fig. 3 shows the properties of the embedded inductor as a function of the gap H_g between rectangular helix and ground plane. The effective inductance L_{eff} of the structure can be adjusted by increasing and reducing the shunt parasitic capacitor C_g, which is related to H_g. Moving the ground plane closer to the inductor footprint increases C_g, thereby cancelling part of the

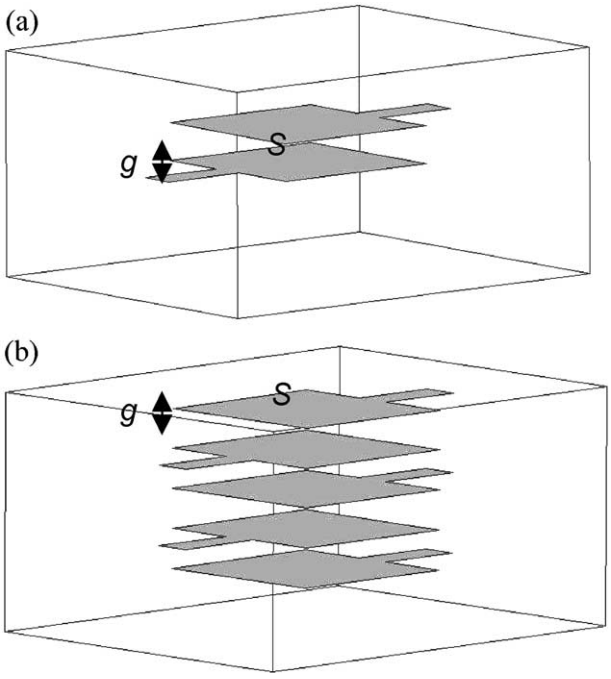

Fig. 4. The structure of the conventional MIM capacitor (a) and the multiple MIM capacitor (b).

effective inductance L_{eff} and making Q higher. On the other hand, moving the ground plane further from structure reduces C_g and increases L_{eff}. The reduction in L_{eff} consequently increases the self resonance frequency (SRF) and reduces the peak value of Q. As indicated in Fig. 3, two full-turn inductors with H_g of 0.2 mm and 1.0 mm exhibit L_{eff} of 3.2 and 7.2 nH with the Q of 53 and 81 at 2.0 GHz and SRF of 4.6 and 3.5 GHz, respectively.

Fig. 4 shows the structures of the conventional metal–insulator–metal (MIM) capacitor and the embedded capacitor. The MIM structure consisting of a dielectric layer sandwiched between two rectangular plates of area S in Fig. 4a implements a capacitor with the capacitance given by $C=\varepsilon_0\varepsilon_r S/g$. This MIM capacitor can be miniaturized by a parallel combination of pairs of plates of smaller size, as shown in Fig. 4b. Fig. 5 shows the properties of the capacitor as a function of the number of plates with $S=1.0\times1.0$ mm^2 and $g=0.1$ mm. The reduction in C_{eff} consequently increases the SRF and the value of Q. The multiple MIM capacitor with either two or six plates exhibit C_{eff} of 1.3 and 5.3 pF with the SRF of 4.4 and 2.0 GHz, respectively.

4. Design of the MLC chip LPF

Fig. 6a shows the structure of the MLC chip LPF, which is designed using 100 μm-thick tape with a dielectric constant of 7.8 and a loss tangent of 0.0043. It has a size of $2.0\times1.2\times1.0$ mm^3. The LPF consists of

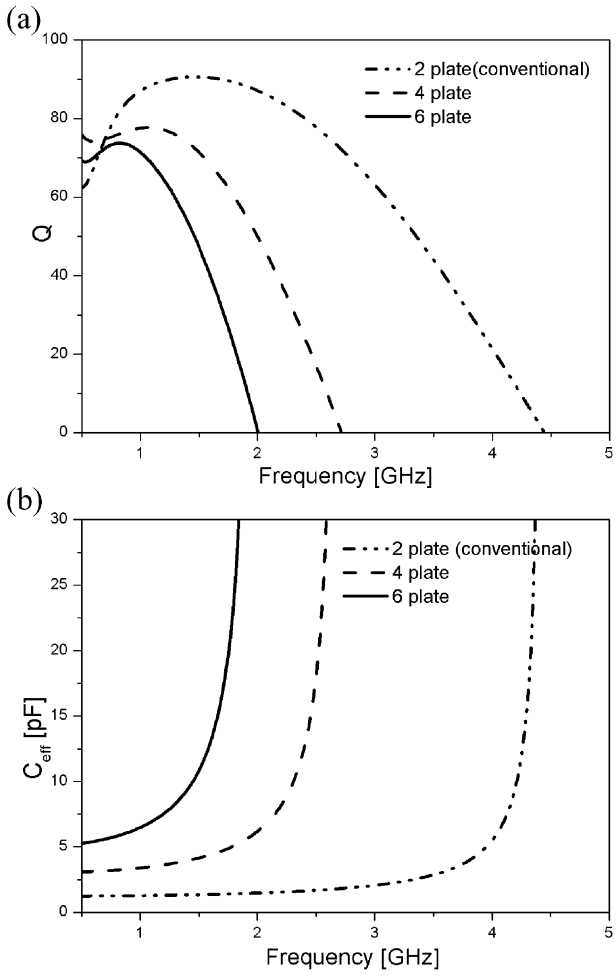

Fig. 5. The frequency characteristics of the multiple MIM capacitor ($S=1.0\times1.0$ mm, $g=0.1$ mm).

three inductors and three capacitors, which are separated by ground planes in order to suppress parasitic couplings, as shown in Fig. 6a. Fig. 6b shows the simulated results for structures shown in Figs. 1 and 6a. An attenuation pole at 3.7 GHz is realized to enhance a skirt characteristic in the rejection band. Table 1 shows the comparison between circuit-simulated and structure-simulated result, for which maximum insertion loss and minimum attenuation of circuit- and structure simulation are 0.1 and 0.5 dB within the passband of 1920–2170 MHz, and 41 and 32 dB in the rejection band at higher than twice cutoff frequency of 2 GHz.

Table 1
Comparison of the circuit-simulated results and structure simulated results

	Passband [MHz]	Insertion loss [dB]	Attenuation [dB]
Circuit	1920–2170	0.1 dB max	41 dB min
Structure	1920–2170	0.5 dB max	32 dB min

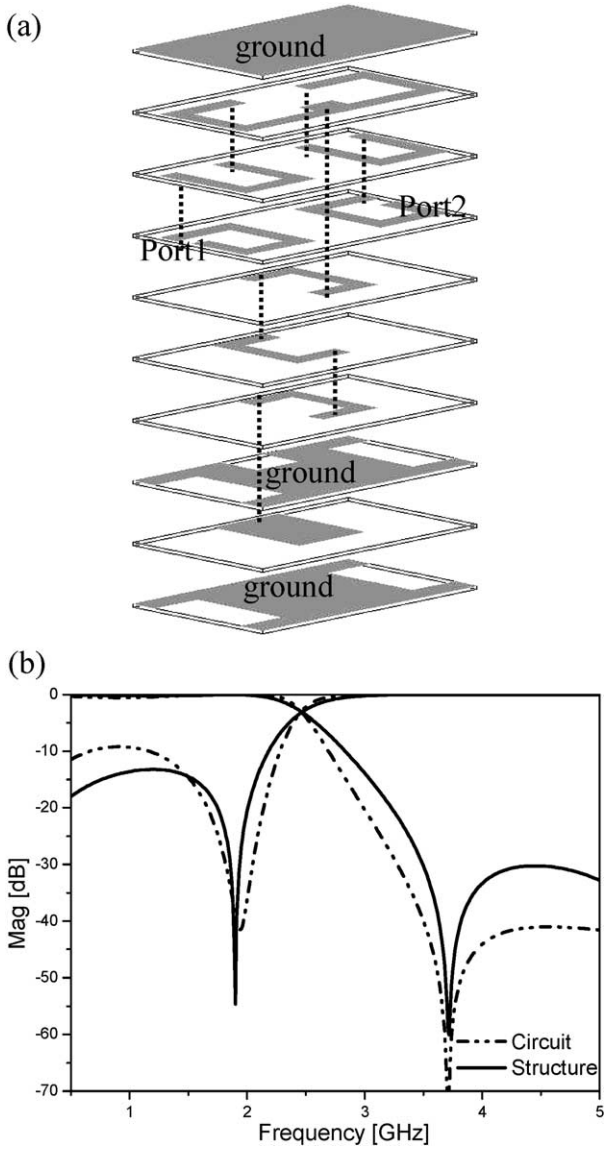

Fig. 6. The structure (a) and simulated results (b) of the MLC chip LPF.

5. Conclusions

The structural analysis of LTCC-based passive components (3D rectangular helical inductors and parallel-plate capacitors) is reported for the design of a small MLC chip LPF. The LPF has small size ($2.0\times1.2\times1.0$ mm^3) uses dielectric material ($\varepsilon_r = 7.8$) and lumped passives, and achieves high attenuation(< -30 dB) by realizing an attenuation pole at 3.7 GHz. The library incorporates the topologies of compact inductor and capacitor yielding a Q as high as 81 at 2 GHz and the corresponding SRF of 3.5 GHz for a 7.2 nH inductor. The Chebyshev lowpass filter was designed with a cutoff frequency of 2 GHz band and a passband ripple of 0.1 dB.

References

1. Chang, K., *RF and Microwave Wireless Systems*. John Wiley and Sons, New York, 2000.
2. Golio, M., *The RF and Microwave Handbook*. CRC Press, Florida, 2001.
3. Sutono, A., Heo, D. H., Chen, Y. E. and Laskar, J., High-Q LTCC-based passive library for wireless system-on-package (SOP) module development. *IEEE Trans. Microwave Theory Tech.*, 2001, **49**, 1715–1724.
4. Ishizaki, T., Uwano, T. and Miyake, H., An extended configuration of a stepped impedance comb-line filter. *IEICE Trans. Electron.*, 1996, **E79-C**, 671–678.
5. Sim, S. H., Kang, C. Y., Yoon, S. J., Yoon, Y. J. and Kim, H. J., Broadband multilayer ceramic chip antenna for handsets. *Electron. Lett.*, 2002, **38**, 205–207.
6. Lew, D. W., Park, J. S., Ahn, Dal., Kang, N. K., Yoo, C. S. and Lim, J. B., A design of the ceramic chip balun using the multilayer configuration. *IEEE Trans. Microwave Theory Tech.*, 2001, **49**, 220–224.
7. Sheen, J. W., LTCC-MLC duplexer for DCS-1800 IEEE Trans. *Microwave Theory Tech.*, 1999, **47**, 1883–1890.
8. Matthaei, G. L., Young, L. and Jones, E. M. T., *Microwave Filters, Impedance-Matching Networks, and Coupling Structures*. McGraw-Hill, New York, 1964.